



THE UNIVERSITY *of* EDINBURGH

Edinburgh Research Explorer

## Cluster analysis of p53 binding site sequences reveals subsets with different functions

### Citation for published version:

Lim, J-H, Latysheva, NS, Iggo, RD & Barker, D 2016, 'Cluster analysis of p53 binding site sequences reveals subsets with different functions' *Cancer Informatics*, pp. 199-209. DOI: 10.4137/CIN.S39968

### Digital Object Identifier (DOI):

[10.4137/CIN.S39968](https://doi.org/10.4137/CIN.S39968)

### Link:

[Link to publication record in Edinburgh Research Explorer](#)

### Document Version:

Peer reviewed version

### Published In:

Cancer Informatics

### General rights

Copyright for the publications made accessible via the Edinburgh Research Explorer is retained by the author(s) and / or other copyright owners and it is a condition of accessing these publications that users recognise and abide by the legal requirements associated with these rights.

### Take down policy

The University of Edinburgh has made every reasonable effort to ensure that Edinburgh Research Explorer content complies with UK legislation. If you believe that the public display of this file breaches copyright please contact [openaccess@ed.ac.uk](mailto:openaccess@ed.ac.uk) providing details, and we will remove access to the work immediately and investigate your claim.



1 **Cluster analysis of p53 binding site sequences reveals**  
2 **subsets with different functions**

3  
4  
5  
6  
7 Ji-Hyun Lim<sup>1,2,3</sup>, Natasha S. Latysheva<sup>1,4</sup>, Richard D. Iggo<sup>2,5</sup> and Daniel Barker<sup>1,6,\*</sup>  
8  
9  
10  
11

12 <sup>1</sup>School of Biology, University of St Andrews, St Andrews, Fife, KY16 9TH, UK.  
13

14 <sup>2</sup>School of Medicine, University of St Andrews, Fife, KY16 9TF, UK.  
15

16 <sup>3</sup>Current address: Alacris Theranostics GmbH, Fabeckstraße 60-62, D-14195 Berlin,  
17 Germany.

18 Email: j.lim@alacris.de  
19

20 <sup>4</sup>Current address: MRC Laboratory of Molecular Biology, Francis Crick Avenue,  
21 Cambridge Biomedical Campus, Cambridge, CB2 0QH, UK.

22 Email: natashal@mrc-lmb.cam.ac.uk  
23

24 <sup>5</sup>INSERM Unit U1218, University of Bordeaux, Institut Bergonie, 229 Cours de l'Argonne,  
25 33076 Bordeaux, France.

26 Email: R.Iggo@bordeaux.unicancer.fr  
27

28 <sup>6</sup>Current address: Institute of Evolutionary Biology, University of Edinburgh,  
29 Charlotte Auerbach Road, The Kings Buildings, Edinburgh, EH9 3FL, UK.

30 Email: Daniel.Barker@ed.ac.uk  
31

32 \*To whom correspondence should be addressed.

33 Email: Daniel.Barker@ed.ac.uk

34 Tel: + 44 (0)131 651 7812.

35 **ABSTRACT**

36

37 p53 is an important regulator of cell cycle arrest, senescence, apoptosis and metabolism, and  
38 is frequently mutated in tumours. It functions as a tetramer, where each component dimer  
39 binds to a decameric DNA region known as a response element. We identify p53 binding site  
40 subtypes and examine the functional and evolutionary properties of these subtypes. We start  
41 with over 1700 known binding sites and, with no prior labelling, identify two sets of response  
42 elements by unsupervised clustering. When combined they give rise to three types of p53  
43 binding site. We find that probabilistic and alignment-based assessments of cross-species  
44 conservation show no strong evidence of differential conservation between types of binding  
45 site. In contrast, functional analysis of the genes most proximal to the binding sites provides  
46 strong bioinformatic evidence of functional differentiation between the three types of binding  
47 site. Our results are consistent with recent structural data identifying two conformations of the  
48 L1 loop in the DNA binding domain, suggesting that they reflect biologically meaningful groups  
49 imposed by the p53 protein structure.

50

51

52 **KEYWORDS**

53

54 p53, transcription factor, protein-DNA interaction, DNA sequence, cluster analysis, function,  
55 conservation, human genome

56

57

58 **INTRODUCTION**

59

60 The p53 transcription factor is well known for its role in suppressing tumour formation. The wild  
61 type form regulates transcription of genes implicated in cell cycle control, apoptosis and  
62 senescence.<sup>1</sup> Common oncogenic p53 mutants either induce a loss of these tumour  
63 suppressor functions or acquire properties that promote cell proliferation, invasion, and  
64 metastasis.<sup>2,3</sup> However, it is increasingly recognised that p53 has a plethora of functions  
65 mediated by a wide range of target genes, often with little or no connection to its 'classical'  
66 roles in cell cycle control and cell death.<sup>4</sup> These functions include metabolic reprogramming,  
67 stem cell maintenance, autophagy, and response to oxidative stress.<sup>5,6</sup> There are perhaps 300-  
68 3000 functional p53 binding sites in the human genome.<sup>7,8,9</sup> p53 binds to these sites as a  
69 homotetrameric 'dimer of dimers', where each dimer interacts with a redundant, approximately  
70 palindromic, decameric DNA motif called the p53 response element (RE).<sup>10,11,12,13,14</sup> The two

71 REs that bind to a full tetramer are either directly adjacent or separated by a few base  
72 pairs.<sup>4,15,16</sup>

73

74 The best characterised p53 REs are typically found either near the promoters or in the first  
75 introns of target genes<sup>17</sup> and are approximately summarized by the 10-base pattern  
76 RRRCWWGYYY<sup>15</sup>, where 'R' indicates A or G, 'W' indicates A or T and 'Y' indicates C or T. In  
77 the ambiguous positions, not all residues are equally frequent; furthermore, other sequence  
78 variations exist. This flexibility suggests the hypothesis that different types of RE could mediate  
79 different biological processes, regulated by p53 with different binding specificities due to  
80 variable intrinsic sequence affinities,<sup>18,19,20</sup> different post-translational modifications, or by  
81 being in complex with different cofactors. Different biological functions might be expected to  
82 be subject to different strengths of natural selection, leading to varying rates of evolution of the  
83 associated REs. Indeed, it has been suggested that REs involved in apoptosis and DNA repair  
84 are more poorly conserved across species than those involved in the cell cycle.<sup>21</sup>

85

86 Here, we computationally investigate the existence of subsets of p53 binding site. One could  
87 divide p53 binding sites or REs into subsets based on criteria such as Gene Ontology (GO)  
88 annotation of the nearest gene,<sup>22</sup> and summarize the properties of these subsets. However,  
89 GO – though an important guideline in broad studies of function – reflects a human-imposed  
90 classification of function, is incomplete, and for intergenic binding sites may involve an arbitrary  
91 decision as to which of the two nearest genes is regulated by the site. Instead of beginning  
92 with GO-based subsets, we begin with the DNA sequences of known binding sites. In an  
93 unsupervised clustering procedure, we classify these on the basis of the sequence similarity  
94 of their constituent decameric REs. This allows groups of binding sites to emerge based on  
95 their sequence, without imposing any limitations based on possible functional consequences.  
96 Our procedure also removes the arbitrary effect of the strand of DNA considered. Once formed  
97 on the basis of sequence similarity, we investigate the function of binding site groups, using  
98 both GO annotation and cross-species conservation, on the assumption that groups differing  
99 in one or both of these respects may have functional significance.

100

101 We use this procedure to group the decameric REs into two clusters, arbitrarily labelled 'cluster  
102 1' and 'cluster 2'. Then, given that two REs form a full p53 binding site, three groups of full  
103 binding site are possible: group '1,1' binding sites, consisting of two REs of cluster 1; group  
104 '2,2' binding sites, consisting of two REs of cluster 2; and group '1,2' binding sites, consisting  
105 of one RE of each type. We find evidence of functional differentiation between these binding  
106 site groups, but find no strong evidence of differential evolutionary conservation.

107

108  
109  
110  
111  
112  
113  
114  
115  
116  
117  
118  
119  
120  
121  
122  
123  
124  
125  
126  
127  
128  
129  
130  
131  
132  
133  
134  
135  
136  
137  
138  
139  
140  
141  
142  
143  
144

## **MATERIALS AND METHODS**

### **Input data**

We obtained 1757 p53 binding sites from the literature, as described by Lim et al.<sup>23</sup> These consist of 327 binding sites from Wei et al.,<sup>1</sup> 1422 from Smeenk et al.<sup>7</sup> after excluding a further 123 also present in Wei et al., and eight from Horvath et al.<sup>21</sup>. These 1757 binding sites are given in Supplementary Material.

### **Clustering p53 response elements**

Within a binding site, we label as 'first' the response element (RE) that is nearer to the start of the chromosome in the conventional representation; it is thus an arbitrary property of the strand of the chromosomal sequence being considered. Binding sites were then each split into the two constituent REs, excluding any spacer. To ensure comparable bases were aligned, the 'second' RE was reverse-complemented. All REs were then represented as strings of bases from the base outermost in the binding site (5') on the left, to the innermost base (3') on the right. Redundant sequences were removed, leaving 1724 unique p53 RE sequences (Supplementary Material).

A symmetrical matrix of RE-to-RE Hamming distance was calculated<sup>24</sup>. Exploratory hierarchical clustering of this distance matrix with the unweighted paired-groups method using arithmetic averages (UPGMA)<sup>25</sup> produced varying results when repeated, presumably due to the arbitrary resolution of ties during the clustering procedure<sup>26,27</sup>. For the final clusters presented in this paper, we instead clustered using Ward's method,<sup>28</sup> which minimises an objective function at each stage in the clustering procedure. In typical implementations, the objective function is within-cluster variance, requiring Euclidian distances as input. Before clustering, we transformed the RE-to-RE Hamming distance matrix to Euclidian distance using the 'lingoes' function of the 'ade4' package<sup>29</sup> in R (<http://www.r-project.org>). Clustering with Ward's method was then performed using the 'hclust' function of R.

To divide the REs into subgroups, we drew a phenon line<sup>30</sup> on the Ward's method cluster diagram at a position that split the REs into two sets (i.e.  $k = 2$  clustering). These two primary clusters of REs represent the most inclusive subsets supported by our analysis. We labelled these primary clusters of REs as 'cluster 1' and 'cluster 2'.

145 The robustness of the grouping of REs into primary clusters was assessed using a jackknife  
146 procedure. 1000 subsamples (jackknife replicates), each with a random set of 37% REs  
147 omitted,<sup>31</sup> were generated from the set of 1724 non-redundant p53 RE sequences. Hence,  
148 each replicate consists of a random subset of 1086 REs (63% of the set of nonredundant REs),  
149 sampled without replacement. Using the same procedure as for the analysis of the set of 1724  
150 non-redundant REs, we clustered REs of each replicate at  $k = 2$ . We mapped each of the two  
151 clusters from each replicate to one of the primary clusters from the analysis of the full set of  
152 non-redundant REs. The replicate cluster with the highest proportion of overlap with cluster 1  
153 of the primary clusters was mapped to primary cluster 1, and the other was mapped to primary  
154 cluster 2. As an indication of robustness of the clustering of the 1724 nonredundant REs, a G-  
155 test was used to investigate the correspondence between the assignment of REs to primary  
156 clusters in each jackknife replicate, and the assignment to the primary clusters in the analysis  
157 of the full, non-redundant set of 1724 REs.

158  
159 To investigate the evolutionary relationships of the primary clusters of RE, position weight-  
160 matrices (PWMs) for the RE clusters were compared to known PWMs for p53, p63 and p73  
161 REs from the Transfac database (BioBase Corporation; [http://www.biobase-  
162 international.com/product/transcription-factor-binding-sites](http://www.biobase-international.com/product/transcription-factor-binding-sites)). If presented in Transfac as  
163 counts, binding site PWMs were converted to a frequency representation. Then, frequencies  
164 for each base position within the RE were taken as the mean of the frequencies for the first RE  
165 and for the reverse-complement of the second RE within the binding site. The resulting RE  
166 PWMs represent base frequencies starting from the outermost base of the binding site on the  
167 left (5') to the innermost base (3') on the right. PWMs were visualized as logos using Weblogo<sup>32</sup>  
168 with the nonredundant sequences as input in the case of cluster 1 and cluster 2, and a synthetic  
169 set of 5000 simulated sequences matching the composition of each base position in the RE  
170 PWM in the case of PWMs based on Transfac. Similarities among the innermost 9 bases of  
171 REs (the outermost base was excluded due to its absence in the p73 PWM, M04503), were  
172 quantified using profile-profile alignment scores calculated as the sum of dot-product scores  
173 for the individual base positions<sup>33,34</sup> without adjusting for background frequencies.

174

### 175 **Functional and evolutionary analysis of p53 binding site subtypes**

176

177 Based on the primary cluster membership of the two constituent REs in the un-jackknifed  
178 cluster analysis, we defined three groups of full p53 binding site. Each binding site may be a  
179 '1,1' binding site, consisting of two REs from cluster 1; a '2,2' binding site, consisting of two  
180 REs from cluster 2; or a '1,2' binding site, consisting of one RE from each cluster. In the latter  
181 case, we make no distinction between binding sites in which the RE from cluster 1 comes 'first'

182 and those in which it comes 'second', since this distinction is arbitrary, depending only on which  
183 strand of the double helix is being considered.

184

185 To investigate differential pairing between RE clusters within binding sites, we performed a G-  
186 test for evidence of association between 'cluster 1' and 'cluster 2' REs within the full, redundant  
187 set of 1757 p53 binding sites.

188

189 To test for functional differences between the three groups of binding sites ('1,1', '1,2' and '2,2'),  
190 nearest genes were assigned to binding sites as described by Lim et al.<sup>23</sup> Enrichment for GO  
191 biological process terms was performed with PANTHER<sup>35</sup> (<http://www.pantherdb.org>; version  
192 11.0, released 2016-07-15). To test for overlap with hallmark gene sets, Ensembl Gene 85 IDs  
193 were converted to GRCh38.7 Entrez Gene IDs with Biomart then compared to the  
194 h.all.v5.1.entrez.gmt hallmark gene set in the Molecular Signatures Database<sup>36</sup> (MSigDB v5.1,  
195 January 2016 release; <http://software.broadinstitute.org/gsea/msigdb/annotate.jsp>).

196

197 Conservation levels for the three sets of binding site were first investigated using PhastCons  
198 scores,<sup>37</sup> which quantify negative selection by using a hidden Markov model-based method to  
199 estimate the probability that each nucleotide in a multiple alignment forms part of a conserved  
200 sequence element. PhastCons conservation scores take into account the conservation of  
201 neighbouring bases, which makes PhastCons scores a natural choice for detecting stretches  
202 of conserved sequence, such as p53 binding sites. We obtained PhastCons scores which  
203 represent levels of conservation (ranging 0 to 1, where higher values indicate higher  
204 conservation) across the following ten primate species: *Homo sapiens* (genome assembly  
205 hg19), *Pan troglodytes* (panTro2), *Gorilla gorilla* (gorGor1), *Pongo abelii* (ponAbe2), *Macaca*  
206 *mulatta* (rheMac2), *Papio hamadryas* (papHam1), *Callithrix jacchus* (calJac1), *Tarsius syrichta*  
207 (tarSyr1), *Microcebus murinus* (micMur1), and *Otolemur garnetti* (otoGar1). The PhastCons  
208 scores for every p53 binding site (as the average across all constituent base pairs within the  
209 site) were extracted using the UCSC table browser function ([http://genome.ucsc.edu/cgi-  
210 bin/hgTables](http://genome.ucsc.edu/cgi-bin/hgTables)). For comparison, a background level of conservation was estimated from a pre-  
211 calculated, genome-wide phastCons score set downloaded from UCSC  
212 (<http://hgdownload.cse.ucsc.edu/goldenpath/hg19/phastCons46way/primates>). Random  
213 segments of the human genome, for which PhastCons scores were available, were sampled  
214 with replacement 10,000 times. Lengths of these segments were sampled from an empirical  
215 distribution, estimated from the lengths of the known p53 binding sites. Conservation scores  
216 for the various binding site groups ('1,1', '1,2' and '2,2') and the background were compared  
217 using Kruskal-Wallis (KW) tests, a non-parametric equivalent of ANOVA.

218



219 Secondly, as an additional approach to test binding site conservation, alignments of genomic  
220 regions containing p53 binding sites were extracted using the Ensembl Perl API.<sup>38</sup> Genomic  
221 coordinates of p53 binding sites in the three groups were first converted to hg19 coordinates,  
222 and the evolutionary conservation of the binding sites was assessed by calculating average  
223 percentage identities in three types of alignments. The alignments used were, firstly, the LastZ-  
224 net<sup>39</sup> pairwise alignment of *Homo sapiens* (GRCh37) versus *Pan troglodytes* (CHIMP2.1.4);  
225 secondly, the EPO<sup>40,41</sup> multiple alignment of six primates (*Homo sapiens*, *Gorilla gorilla*, *Pan*  
226 *troglodytes*, *Pongo abelii*, *Macaca mulatta*, *Callithrix jacchus*); and thirdly, the EPO alignment  
227 of 15 eutherian mammals (*Homo sapiens*, *Gorilla gorilla*, *Pan troglodytes*, *Pongo abelii*,  
228 *Macaca mulatta*, *Callithrix jacchus*, *Mus musculus*, *Rattus norvegicus*, *Oryctolagus cuniculus*,  
229 *Equus caballus*, *Felis catus*, *Canis familiaris*, *Sus scrofa*, *Bos taurus*, *Ovis aries*).

230

231 Methods are further discussed in the Supplementary Material.

232

233

## 234 **RESULTS**

235

### 236 **Clusters of p53 response elements and binding sites**

237

238 Ward's method clustering of nonredundant p53 REs based on Euclidian distance led to primary  
239 clusters of size 410 and 1314, which we designate 'cluster 1' and 'cluster 2', respectively  
240 (Figure 1; Figure 2).

241

242 The spread of results among jackknife replicates is summarized in Table 1. Table 1 shows  
243 very strong evidence of association between the original classification of REs into two clusters  
244 and the classification of REs into two clusters in jackknife replicates. In the majority of jackknife  
245 replicates, REs are assigned to the same primary cluster as in the analysis of the un-jackknifed  
246 set of 1724 nonredundant REs (Figure S1). Hence, the two primary clusters (Figure 1) are  
247 based on a pervasive difference that is present throughout the dataset.

248

249 For the full set of 1757 binding sites, 140 were in group '1,1' (consisting of two REs from cluster  
250 1); 687 were in group '1,2' (consisting of one RE from each cluster); and 930 were in group  
251 '2,2' (consisting of two REs from cluster 2). Given the relative sizes of cluster 1 and cluster 2,  
252 these counts are not statistically significantly different from expectations under a null  
253 hypothesis of independent assignment of RE clusters to binding sites ( $G = 0.689$ ,  $df = 2$ ,  $p =$   
254  $0.709$ ).

255



## 256 **Comparison of response element clusters with existing PWMs**

257

258 When compared to PWMs for REs from known p53, p63 and p73 binding sites derived from  
259 Transfac, our cluster 1 REs are most similar to the p53 RE, then to the p73 RE. Both of our  
260 RE clusters are most similar to the Transfac p53 RE, then to the p73 RE, and least similar to  
261 the p63 RE (Table 2). Cluster 1 and the Transfac-based PWM for the p53 RE show a stronger  
262 CCC homopolymer in the three bases innermost in the binding site than do cluster 2, the p63  
263 RE or the p73 RE (Figure 2).

264

## 265 **Functional analysis of binding site groups**

266

267 To identify potential differences in the function of genes near the different classes of binding  
268 site, we measured the overlap with genes defining 50 hallmark biological processes in the  
269 Molecular Signatures Database (MSigDB)<sup>36</sup>. The hallmark most strongly associated with all  
270 three of our binding site groups was 'genes involved in p53 pathways and networks', confirming  
271 the validity of the approach (Table S1). The results for the other hallmarks are shown visually  
272 in Figure 3, with numerical details in Table S1. The main functional difference found between  
273 binding site groups is that group '2,2' is associated with a much broader set of functions. Group  
274 '1,1' is mainly associated with signal transduction pathways, particularly pro-survival and  
275 oncogenic pathways. Group '1,2' had an intermediate phenotype, functionally broader than  
276 group '1,1' but not as broad as group '2,2'. GO enrichment analysis confirmed that group '2,2'  
277 is associated with a much broader set of functions than the other two groups (Tables S2-S4).  
278 Based on these analyses, we conclude that a switch between '1,1' and '2,2' modes of DNA  
279 binding would change the spectrum of biological functions activated by p53.

280

## 281 **Conservation of binding site groups**

282 The conservation of binding sites in each group was first assessed using PhastCons scores,  
283 which are base-by-base probabilities of a given nucleotide belonging to an evolutionarily  
284 conserved element. The distributions of PhastCons scores for the three classes of binding  
285 sites, as well as the conservation scores across the length-matched genomic background, are  
286 shown in Figure 4. There is no statistically significant difference between conservation scores  
287 across the three groups of binding site (KW  $\chi^2 = 2.49$ ,  $df = 2$ ,  $p = 0.288$ ). Conservation of  
288 binding sites and flanking regions was also assessed (Figure S2). No statistically significant  
289 differences in evolutionary conservation were found when sequences flanking the binding sites  
290 were included by adding 50 base pairs on each side of a binding site (forming ~110 bp regions,  
291 i.e. 100 bp flanking regions; KW  $\chi^2 = 0.052$ ,  $df = 2$ ,  $p = 0.974$ ). Similarly, no statistically  
292 significant difference was found when longer, 1000 bp flanking regions were included (forming

293 ~1010 bp regions; KW  $\chi^2 = 1.78$ ,  $df = 2$ ,  $p = 0.410$ ). The difference between conservation  
294 scores for all p53 binding sites (mean = 0.176, median = 0.044) and background levels of  
295 genome conservation (mean = 0.127, median = 0.041) was also not statistically significant  
296 (KW  $\chi^2 = 0.100$ ,  $df=2$ ,  $p=0.752$ ). Similarly, no statistically significant differences were found  
297 when separately comparing the conservation of each binding site to the background level of  
298 conservation.

299

300 The distribution of PhastCons conservation scores in both the p53 binding site and genomic  
301 background sequences appears slightly bimodal (Figure 4). The second peak, representing  
302 the highest observed conservation levels, is more pronounced for binding sites than for the  
303 genomic background. We find that 102 binding sites have PhastCons conservation scores  
304 greater than or equal to 0.90, representing 5.9% of all binding sites, but only 195 (2.0%) of  
305 length-matched background genomic regions fall into this highly conserved category. This  
306 constitutes strong evidence that binding sites may have a larger subset of highly conserved  
307 sequences (G-test vs genomic background as an extrinsic null hypothesis;  $G = 73.45$ ,  $df = 1$ ,  
308  $p < 2.2 \times 10^{-16}$ ). Further examining the highly conserved p53 subset, we find that group '1,1'  
309 sites may be slightly overrepresented. Group '1,1' represents 8.1% of all binding sites, but  
310 constitutes 9.8% of the highly conserved subset, though this difference is not statistically  
311 significant (G-test on 2x2 contingency table;  $G = 0.42$ ,  $df = 1$ ,  $p = 0.52$ ). Applying a less  
312 stringent (but high) conservation score cut-off of 0.8, 141 binding sites (8.2%) are above the  
313 cut-off, compared to the genomic background level of 2.9% (G-test vs extrinsic null hypothesis;  
314  $G = 92.34$ ,  $df = 1$ ,  $p < 2.2 \times 10^{-16}$ ), and the proportion of the conserved subset included in group  
315 '1,1' rises to 12.1%, though this difference remains statistically non-significant (G-test on 2x2  
316 contingency table;  $G = 2.93$ ,  $df = 1$ ,  $p = 0.087$ ).

317

318 The finding of no strong evidence that p53 binding sites are more conserved than background  
319 genomic sequences is in accord with the observation that transcription factor binding sites  
320 show high evolutionary turnover, both in general<sup>42</sup> and particularly for p53.<sup>21</sup> There was no  
321 strong evidence of a difference in conservation between the functionally broader group '2,2'  
322 and the others (group '1,1' with group '1,2' mean = 0.177, median = 0.046; group '2,2' mean =  
323 0.175, median = 0.041; KW  $\chi^2 = 0.429$ ,  $df = 1$ ,  $p = 0.512$ ).

324

325 As an alternative means to analyse binding site conservation, three sets of multiple alignments  
326 were examined to study p53 binding site sequence divergence over increasingly long spans  
327 of evolutionary time (chimp-human, primate, and eutherian mammal; Figure S3).  
328 Overwhelmingly, these alignments support the PhastCons-based conclusion of no differential  
329 conservation between binding site groups (Table 3). The sole conservation differences close

330 to the conventional cut-off for statistical significance for a single test ( $p < 0.05$ ) occur in the  
331 chimp-human comparison: group '1,1' binding sites are more highly conserved between  
332 humans and chimps than both group '1,2' ( $p = 0.051$ ) and group '2,2' ( $p = 0.040$ ; Table 3). This  
333 may be taken as weak evidence for the conservation of group '1,1' p53 binding site functionality  
334 between chimps and humans, or equivalently, the relative divergence of p53 binding sites  
335 related to non-canonical functions (i.e. those containing cluster 2 REs). However, the statistical  
336 significance is borderline and may be misleading due to multiple testing. Higher conservation  
337 of group '1,1' binding sites was not observed in the primate alignments or in the mammal  
338 alignments (Table 3).

339

340

## 341 **DISCUSSION**

342

343 We have shown that subtle differences in p53 binding site functionality can be identified by  
344 clustering the constituent decamers on the basis of sequence similarity. We obtained a robust  
345 grouping of decamers into two major clusters. These two clusters of decamers can give rise to  
346 three groups of binding site, each composed of one of the three possible combinations of  
347 decamer. The frequencies of specific pairings of decamers from the two clusters into binding  
348 sites show no strong difference compared to random expectation, and we find no appreciable  
349 difference in conservation compared to background genome conservation levels. Furthermore,  
350 the three binding site groups also showed little evidence of differential conservation between  
351 themselves, with the strongest evidence hinting at relatively strong chimp/human conservation  
352 of group '1,1' binding sites, though with only borderline statistical significance. However, we  
353 find that genes near '2,2' sites have a much broader range of functions than genes near '1,1'  
354 and '1,2' sites, (Figure 3 and Tables S1-S4). Combined with the robustness of the RE clusters  
355 demonstrated by jackknifing, and with results from earlier studies (discussed below), we  
356 conclude that switching p53 from a '1,1' to a '2,2' mode of binding would substantially change  
357 the functional consequences of p53 activation.

358

359 Our results confirm a long-standing suspicion that p53 binding sites are not simply duplicated  
360 copies of a symmetrical RRRCWWGYYY decamer. Instead, the REs in cluster 1 are C-rich in  
361 the final three positions, which correspond to the innermost positions in the middle of a full  
362 20mer (or larger) binding site. Because of the way we report the decamer sequences, '1,1'  
363 binding sites will tend to have the sequence 'CCCGGG' at the centre of the 20mer. This is the  
364 sequence that was found in the original SELEX study that first defined the p53 binding site.<sup>43</sup>  
365 Shortly thereafter we showed that mutations in the L1 loop alter the affinity and specificity of  
366 DNA binding,<sup>18</sup> but an understanding of the mechanism had to wait until the Halazonetis group

367 discovered that the L1 loop in *C. elegans* p53 contains a small alpha helix.<sup>11</sup> They went on to  
368 show that the L1 loop in human p53 can form the same alpha helix.<sup>44</sup> The lysine 120 DNA  
369 contact residue lies at the tip of the loop. Accordingly, formation of the alpha helix retracts the  
370 lysine from the DNA. The discovery that the L1 loop can adopt two different conformations  
371 immediately suggests an explanation for the asymmetry in the cluster 1 and cluster 2  
372 sequences in our study. The L1 loop is in the retracted form in the outer p53 subunits in the  
373 tetramer.<sup>44,45,46</sup> In this form lysine 120 can not reach into the major groove to contact the bases,  
374 so the sequence is less constrained. In contrast, the loop is in the extended form in the inner  
375 two subunits, allowing lysine 120 to forms hydrogen bonds with the bases in the major groove.  
376 The hydrogen bonds between the side chains of lysine 120, cysteine 277 and arginine 280  
377 and the DNA are shown as yellow dotted lines in Figure 5A. The L1 loop is shown in the  
378 extended form in Figure 5B, and in the retracted state in Figure 5C. Switching to the extended  
379 conformation allows induced fitting of the protein to the DNA when the correct sequence is  
380 present.<sup>44,45</sup> It is likely that the L1 loop adopts many different conformations while searching  
381 for the correct sequence and that, thanks to induced fitting, this leads to important differences  
382 in the kinetics of binding that depend on the sequence.<sup>44,45</sup> In addition to the inner-outer  
383 asymmetry caused by changes in the conformation of the L1 loop there are differences  
384 between the hydrogen bonds formed, depending on the exact sequence at positions 8 and 9  
385 in the decamer: cysteine 277 forms a hydrogen bond with either O4 of thymine or N4 of  
386 cytosine at position 8; lysine 120 forms hydrogen bonds with N7 and O6 of guanine but only  
387 N7 of adenine at position 9; and hydrophobic and van de Waals forces from alanine 276 and  
388 cysteine 277 stabilise the C5 methyl group in T at position 8.<sup>10,44,45</sup> Taken together, these data  
389 would lead us to expect p53 to bind with decreasing affinity to '1,1', '1,2', and '2,2' sites.  
390 Hallmark analysis reveals a preference for prosurvival and oncogenic signalling pathways for  
391 '1,1' sites (Figure 3). This is consistent with old suggestions that p53 promotes survival early  
392 after activation, and only binds to all of its targets if the signal persists and p53 accumulates.  
393 Originally this was interpreted as a binary switch between cell cycle arrest and apoptotic sites,  
394 with the latter containing only a single decamer<sup>18,20</sup> and having a lower affinity for p53<sup>20,19</sup>, but  
395 the multiplication of p53 functions over time means the effects are likely to be more diverse  
396 and to depend heavily on the cellular context. The most important DNA binding residue in p53  
397 is arginine 280, which forms hydrogen bonds with the G base paired to the invariant C at  
398 position 4 in the pentamer. The corresponding positions in the decamer are 4 (C) and 7 (G).  
399 The pattern in cluster 1, with a stronger preference for G at position 7 than for C at position 4,  
400 is reminiscent of a binding site profile identified by Veprintsev and Fersht.<sup>8</sup> Interestingly,  
401 acetylation of lysine 120<sup>47,48</sup> negated the difference.<sup>49</sup> In addition to acetylation of K120, the  
402 cell can manipulate the sequence specificity of p53 through multiple mechanisms, for example  
403 binding to Hzf and ASPP proteins.<sup>50,51</sup> Indeed, many publications have described plausible

404 regulatory mechanisms based on post-translational modifications and protein-protein  
405 interactions (reviewed by Carvajal and Manfredi<sup>52</sup>) that could explain the differences we have  
406 found by clustering of p53 binding sites. Given the elegant structural studies from the  
407 Halazonetis group cited above, we suspect that these regulatory mechanisms converge on the  
408 L1 loop and switch p53 from a '1,1' to a '2,2' mode of binding.

409

410 In conclusion, we have shown that p53 binding sites can be classified into groups that may  
411 reflect the different modes of DNA binding that have been described in structural studies.  
412 Integration of sequence-based clustering with data on post-translational modification, cofactor  
413 binding and changes in the structure of the DNA binding domain is a promising direction for  
414 future research.

415

416

## 417 **ACKNOWLEDGEMENTS**

418

419 We acknowledge the financial support of the University of St Andrews School of Medicine and  
420 a BBSRC Doctoral Training Grant [BB/D526845/1] (studentship to J.-H.L.); The University of  
421 St Andrews Undergraduate Research Internship Programme (award to N.L.); and the French  
422 National Research Agency [ANR grant ANR-08-CEXC-016-01 to R.I.].

423

424

## 425 **AUTHOR CONTRIBUTIONS**

426

427 Conceived and designed the analyses: J-HL, NSL, RDI, DB. Performed the analysis: J-HL,  
428 NSL, RDI, DB. Wrote the manuscript: J-HL, NSL, RDI, DB. Agree with manuscript results and  
429 conclusions: J-HL, NSL, RDI, DB. All authors read and approved of the final manuscript.

430

431

## 432 **REFERENCES**

433

434 1. Wei CL, Wu Q, Vega VB, et al. A global map of p53 transcription-factor binding sites in the  
435 human genome. *Cell*. 2006;124:207-19.

436

437 2. Muller PAJ, Vousden KH. p53 mutations in cancer. *Nat. Cell Biol.* 2013;15:2-8.

438

439 3. Muller PAJ, Vousden KH. Mutant p53 in cancer: new functions and therapeutic opportunities.  
440 *Cancer Cell*. 2014;25:304-317.

441  
442 4. Menendez D., Inga A, Resnick MA. The expanding universe of p53 targets. *Nat. Rev. Cancer.*  
443 2009;9:724-37.  
444  
445 5. Bieging KT, Mello SS, Attardi LD. Unravelling mechanisms of p53-mediated tumour  
446 suppression. *Nat. Rev. Cancer.* 2014;14:359-70.  
447  
448 6. Hager KM, Gu W. Understanding the non-canonical pathways involved in p53-mediated  
449 tumor suppression. *Carcinogenesis.* 2014;35:740-6.  
450  
451 7. Smeenk L, van Heeringen SJ, Koeppel, M., et al. Characterization of genome-wide p53-  
452 binding sites upon stress response. *Nucleic Acids Res.* 2008;36:3639-54.  
453  
454 8. Veprintsev DB, Fersht AR. Algorithm for prediction of tumour suppressor p53 affinity for  
455 binding sites in DNA. *Nucleic Acids Res.* 2008;36:1589-98.  
456  
457 9. Wang B, Niu D, Lam TH, Xiao Z, Ren EC. Mapping the p53 transcriptome universe using  
458 p53 natural polymorphs. *Cell Death Differ.* 2014;21:521-32.  
459  
460 10. Cho Y, Gorina S, Jeffrey PD, Pavletich NP. Crystal structure of a p53 tumor suppressor-  
461 DNA complex: understanding tumorigenic mutations. *Science.* 1994;265:346-55.  
462  
463 11. Huyen Y, Jeffrey PD, Derry WB, et al. Structural differences in the DNA binding domains  
464 of human p53 and its *C. elegans* ortholog Cep-1. *Structure.* 2004;12:1237-43.  
465  
466 12. Kitayner M, Rozenberg H, Kessler N, et al. Structural basis of DNA recognition by p53  
467 tetramers. *Mol. Cell.* 2006;22:741-53.  
468  
469 13. Ho WC, Fitzgerald MX, Marmorstein R. Structure of the p53 core domain dimer bound to  
470 DNA. *J. Biol. Chem.* 2006;281:20494-502.  
471  
472 14. Joerger AC, Fersht AR. Structural biology of the tumor suppressor p53. *Annu. Rev.*  
473 *Biochem.* 2008;77:557-82.  
474  
475 15. El-Deiry WS, Kern SE, Pietenpol JA, Kinzler KW, Vogelstein B. Definition of a consensus  
476 binding site for p53. *Nat. Genet.* 1992;1:45-9.  
477

- 478 16. Riley T, Sontag E, Chen P, Levine A. Transcriptional control of human p53-regulated genes.  
479 *Nat. Rev. Mol. Cell Biol.* 2008;9:402-12.  
480
- 481 17. Brady CA, Attardi LD. p53 at a glance. *J. Cell Sci.* 2010;123:2527-2532.  
482
- 483 18. Freeman J, Schmidt S, Scharer E, Iggo R. Mutation of conserved domain II alters the  
484 sequence specificity of DNA binding by the p53 protein. *EMBO J.* 1994;13:5393-400.  
485
- 486 19. Ludwig RL, Bates S, Vousden KH. Differential activation of target cellular promoters by  
487 p53 mutants with impaired apoptotic function. *Mol. Cell. Biol.* 1996;16:4952-60.  
488
- 489 20. Saller E, Tom E, Brunori M, et al. Increased apoptosis induction by 121F mutant p53.  
490 *EMBO J.* 1999;18:4424-4437.  
491
- 492 21. Horvath MM, Wang X, Resnick MA, Bell DA. Divergent evolution of human p53 binding  
493 sites: cell cycle versus apoptosis. *PLoS Genet.* 2007;3:e127.  
494
- 495 22. Gene Ontology Consortium. Gene ontology annotations and resources. *Nucleic Acids Res.*  
496 2013;41:D530-5.  
497
- 498 23. Lim J-H, Iggo RD, Barker D. Models incorporating chromatin modification data identify  
499 functionally important p53 binding sites. *Nucleic Acids Res.* 2013;41:5582-93.  
500
- 501 24. Hamming RW. Error detecting and error correcting codes. *Bell System Technical*  
502 *Journal.* 1950;29:147-60.  
503
- 504 25. Sokal RR, Michener CD. A statistical method for evaluating systematic  
505 relationships. *University of Kansas Scientific Bulletin.* 1958;28:1409-38.  
506
- 507 26. Backeljau T, De Bruyn L, De Wolf H, Jordaens K, Van Dongen S, Winnepenickx W.  
508 Multiple UPGMA and neighbour-joining trees and the performance of some computer  
509 packages. *Mol. Biol. Evol.* 1996;13:309-13.  
510
- 511 27. Scherma D, Podani J, Erős T. Measuring the contribution of community members to  
512 functional diversity. *Oikos.* 2009;118:961-71.  
513



- 514 28. Ward JH. Hierarchical grouping to optimize an objective function. *J. Am. Stat. Assoc.*  
515 1963;58:236-44.  
516
- 517 29. Dray S, Dufour AB. The ade4 package: implementing the duality diagram for ecologists. *J.*  
518 *Stat. Softw.* 2007;22:1-20.  
519
- 520 30. Sneath PHA, Sokal RR. *Numerical taxonomy: The Principles and Practice of Numerical*  
521 *Classification*. San Francisco: W.H. Freeman; 1973.  
522
- 523 31. Farris JS, Albert VA, Källersjö M, Lipscomb D, Kluge AG. Parsimony jackknifing  
524 outperforms neighbor joining. *Cladistics*. 1996;12:99-124.  
525
- 526 32. Crooks GE, Hon G, Chandonia JM, Brenner SE. WebLogo: A sequence logo generator.  
527 *Genome Res.* 2004;14:1188-90.  
528
- 529 33. Ohlson T, Wallner B, Elofsson A. Profile-profile methods provide improved fold-recognition:  
530 a study of different profile-profile alignment methods. *Proteins*. 2004;57:188-97.  
531
- 532 34. Wang G, Dunbrack RL. Scoring profile-to-profile sequence alignments. *Protein Science*.  
533 2004;13:1612-26.  
534
- 535 35. Mi H, Poudel S, Muruganujan A, Casagrande JT, et al. PANTHER version 10: expanded  
536 protein families and functions, and analysis tools. *Nucleic Acids Res.* 2016;44(D1):D336-342.  
537
- 538 36. Subramanian A, Tamayo P, Mootha VK, Mukherjee S, Ebert BL, Gillette M, Paulovich A,  
539 Pomeroy SL, Golub TR, Lander ES, Mesirov JP. Gene set enrichment analysis: A knowledge-  
540 based approach for interpreting genome-wide expression profiles. *Proc. Natl. Acad. Sci. USA*.  
541 2005;102:15545-15550.  
542
- 543 37. Siepel A, Bejerano G, Pedersen JS, et al. Evolutionarily conserved elements in vertebrate,  
544 insect, worm, and yeast genomes. *Genome Res.* 2005;15:1034-50.  
545
- 546 38. Stabenau A, McVicker G, Melsopp C, Proctor G, Clamp M, Birney E. The Ensembl core  
547 software libraries. *Genome Res.* 2004;14:929-33.  
548
- 549 39. Harris RS. Improved pairwise alignment of genomic DNA. Ph.D. Thesis, Pennsylvania  
550 State University; 2007.

551  
552 40. Paten B, Herrero J, Beal K, Fitzgerald S, Birney E. Enredo and Pecan: Genome-wide  
553 mammalian consistency-based multiple alignment with paralogs. *Genome Res.* 2008;18:1814-  
554 28.  
555  
556 41. Paten B, Herrero J, Fitzgerald, S, et al. Genome-wide nucleotide-level mammalian  
557 ancestor reconstruction. *Genome Res.* 2008;18:1829-43.  
558  
559 42. Doniger SW, Fay JC. Frequent gain and loss of functional transcription factor binding sites.  
560 *PLoS Comput. Biol.* 2007;3:e99.  
561  
562 43. Funk WD, Pak DT, Karas RH, Wright WE, Shay JW. A transcriptionally active DNA-binding  
563 site for human p53 protein complexes. *Mol. Cell. Biol.* 1992;12:2866-71.  
564  
565 44. Petty TJ, Emamzadah S, Costantino L, et al. An induced fit mechanism regulates p53 DNA  
566 binding kinetics to confer sequence specificity. *EMBO J.* 2011;30:2167-76.  
567  
568 45. Emamzadah S, Tropa L, Halazonetis TD. Crystal structure of a multidomain human p53  
569 tetramer bound to the natural CDKN1A (p21) p53-response element. *Mol. Cancer Res.*  
570 2011;9:1493-9.  
571  
572 46. Emamzadah S, Tropa L, Vincenti I, Falquet B, Halazonetis TD. Reversal of the DNA-  
573 binding-induced loop L1 conformational switch in an engineered human p53 protein. *J. Mol.*  
574 *Biol.* 2014;426:936-44.  
575  
576 47. Sykes SM, Mellert HS, Holbert MA, Li K, Marmorstein R, Lane WS, McMahon SB.  
577 Acetylation of the p53 DNA-binding domain regulates apoptosis induction. *Mol. Cell.*  
578 2006;24:841-51.  
579  
580 48. Tang Y, Luo J, Zhang W, Gu W. Tip60-dependent acetylation of p53 modulates the  
581 decision between cell-cycle arrest and apoptosis. *Mol. Cell.* 2006;24:827-39.  
582  
583 49. Arbely E, Natan E, Brandt T, et al. Acetylation of lysine 120 of p53 endows DNA-binding  
584 specificity at effective physiological salt concentration. *Proc. Natl. Acad. Sci. U.S.A.*  
585 2011;108:8251-6.  
586  
587 50. Das S, Raj L, Zhao B, Kimura Y, Bernstein A, Aaronson SA, Lee SW. Hzf Determines cell

588 survival upon genotoxic stress by modulating p53 transactivation. *Cell*. 2007;130:624-37.

589

590 51. Samuels-Lev Y, O'Connor DJ, Bergamaschi D, Trigiante G, Hsieh JK, Zhong S, Campargue I,  
591 Naumovski L, Crook T, Lu X. ASPP proteins specifically stimulate the apoptotic function of p53. *Mol.*  
592 *Cell*. 2001;8:781-94.

593

594 52. Carvajal LA, Manfredi JJ. Another fork in the road—life or death decisions by the tumour  
595 suppressor p53. *EMBO Rep*. 2013;14:414-21.

596

597 **TABLES**

598  
599

600 **Table 1.** Contingency table showing the relationship between response element (RE)  
601 classification in the original cluster analysis (Figure 1) and re-classification in jackknife  
602 replicates. A highly statistically significant association was observed between the original  
603 classification of REs into two clusters and the classification of REs into two clusters in jackknife  
604 replicates ( $G = 519.98$ , d.f. = 1,  $p < 2.2 \times 10^{-16}$ ).

605

Counts	Replicate cluster 1	Replicate cluster 2	Totals
<b>Original cluster 1</b>	440	70	510
<b>Original cluster 2</b>	344	870	1214
<b>Totals</b>	784	940	$n = 1724$

606

607

608 **Table 2.** Dot-product alignment scores between PWMs for RE cluster 1, RE cluster 2, and  
609 PWMs for the p53 RE, p63 RE and p73 RE derived from the Transfac database (M01651,  
610 M07138 and M04503). To match the PWM for p73, which has REs of length 9, the first  
611 (outermost) base of the other PWMs was omitted. The alignment score depends both on the  
612 extent of matching between profiles and the extent of ambiguity within profiles, and is not a  
613 metric. Scores are symmetrical and are only given for the bottom-left portion of the table.  
614 Scores can range from a maximum of 9, for two unambiguous 9-base PWMs which perfectly  
615 match, to a minimum of 0.

616

	Cluster 1	Cluster 2	p53 Transfac	p63 Transfac	p73 Transfac
<b>Cluster 1</b>	4.8	.	.	.	.
<b>Cluster 2</b>	4.3	4.7	.	.	.
<b>p53 Transfac</b>	4.9	5	5.5	.	.
<b>p63 Transfac</b>	4.3	4.5	4.8	4.5	.
<b>p73 Transfac</b>	4.5	4.9	5.3	4.7	5.3

617

618

619 **Table 3.** p53 binding site conservation as judged by averaged percentage identities from  
 620 multiple sequence alignments. In each alignment, the mean and median percentage identities  
 621 for the three binding site groups are shown. The distribution of percentage identities in each  
 622 binding site group was pairwise tested against the remaining 2 groups ( $X^2$  = Kruskal-Wallis  $X^2$   
 623 statistic;  $p$  =  $p$  value).

624

	<b>Binding site</b>	<b>Mean</b>	<b>Median</b>	<b>Group '1,1'</b>	<b>Group '1,2'</b>
<b>Chimp-human divergence</b>	Group '1,1'	99.18	100	.	.
	Group '1,2'	98.70	100	$X^2 = 3.82, p = 0.051$	.
	Group '2,2'	98.60	100	$X^2 = 4.21, p = 0.040$	$X^2 = 0.03, p = 0.866$
<b>Primate divergence</b>	Group '1,1'	93.73	95	.	.
	Group '1,2'	92.07	95	$X^2 = 0.85, p = 0.358$	.
	Group '2,2'	92.46	95	$X^2 = 0.97, p = 0.325$	$X^2 = 0.007, p = 0.935$
<b>Eutherian mammal divergence</b>	Group '1,1'	82.52	82.37	.	.
	Group '1,2'	82.72	83.30	$X^2 = 0.21, p = 0.645$	.
	Group '2,2'	82.41	82.41	$X^2 = 0.04, p = 0.842$	$X^2 = 1.56, p = 0.221$

625

626

627 **FIGURE CAPTIONS**

628

629 **Figure 1.** Summary of dendrogram obtained by cluster analysis of the 1724 nonredundant  
630 decamers. For visualization purposes, an arbitrary phenon line was drawn at a height of 38.  
631 The number of sequences in each resulting sub-cluster is shown, along with the logo  
632 summarizing those sequences, with bases ranging from 1 (outermost) to 10 (innermost) in the  
633 binding site. The logo *y*-axis represents information content, with ticks at 1 and 2 bits. The full  
634 dendrogram is available as a file in Newick format in the Supplementary Material.

635

636 **Figure 2.** Sequence logos for (a) cluster 1 REs, (b) cluster 2 REs, (c) p53 Transfac RE, (d) p63  
637 Transfac RE and (e) p73 Transfac RE. Bases range from 1 (outermost) to 9 or 10 (innermost)  
638 in the binding site. (c), (d) and (e) are based on Transfac M01651, M07138 and M04503,  
639 respectively.

640

641 **Figure 3.** Functional enrichment for hallmark biological processes. The genes nearest to the  
642 binding sites were used to create putative target gene lists for each group. The bars in the  
643 figure show the relative enrichment for genes in each hallmark; the dots show the *p*-value  
644 expressed as  $-\log_{10}$ . Only hallmarks for which at least one group gave  $p < 0.0001$  are shown;  
645 within each hallmark missing bars correspond to associations with  $p > 0.01$ . For numerical  
646 details see Table S1. The terms in MSigDB corresponding to the labels are: PI3K,  
647 PI3K\_AKT\_mTOR\_signaling; NFKB, TNFA\_signaling\_via\_NFKB; Hyp, hypoxia; TOR,  
648 mTORC1\_signaling; RAS, KRAS\_signaling\_up; UV, UV\_response\_down; Apo, apoptosis;  
649 EMT, epithelial\_mesenchymal\_transition; ER, estrogen\_response\_early; Inf,  
650 inflammatory\_response; Myo, myogenesis; Gly, glycolysis; IL2, IL2\_STAT5\_signaling; Xeno,  
651 xenobiotic\_metabolism.

652

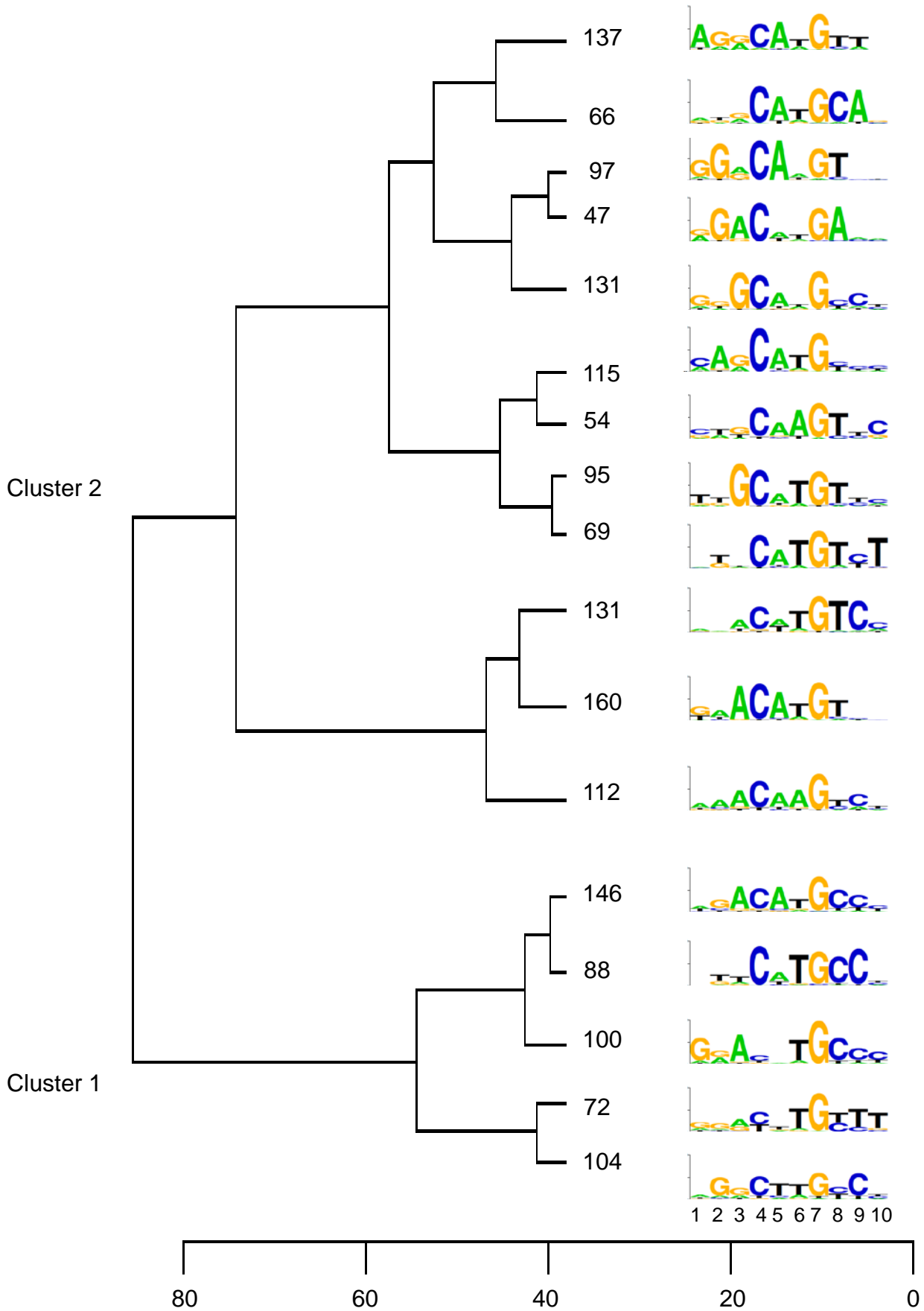
653 **Figure 4.** Histograms of PhastCons evolutionary conservation scores for binding sites in our  
654 p53 binding site group '1,1' ( $n = 140$ ), group '1,2' ( $n = 687$ ), group '2,2' ( $n = 930$ ) and the  
655 genomic background ( $n = 10,000$ ), across 10 species of primates. Dashed lines indicate means  
656 for each group.

657

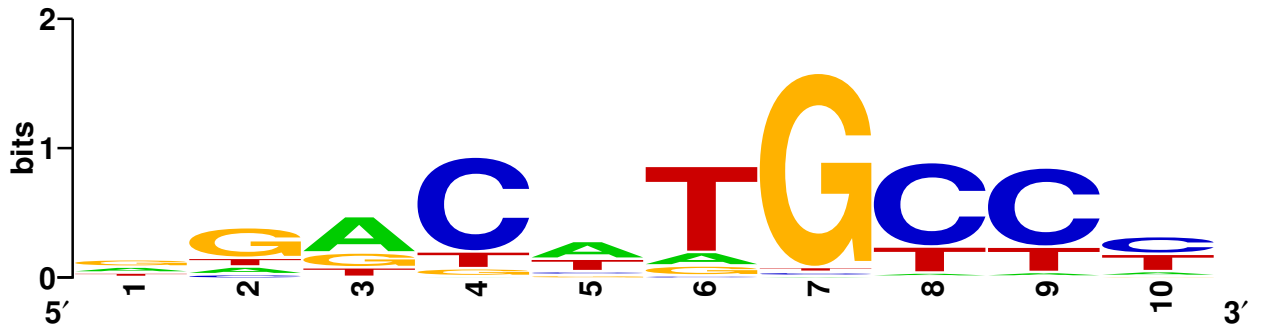
658 **Figure 5.** p53 DNA binding. (A) The p53 loop-sheet-helix is shown in contact with the major  
659 groove of the DNA. Amino acid 120K (cyan) binds to G on the Watson strand; 277C (orange)  
660 binds to T and 280R (red) to G on the Crick strand. Amino acid 120K arises from the tip of the  
661 L1 loop (the green line at the bottom of the figure). Hydrogen bonds are shown as dotted yellow  
662 lines. (B) The L1 loop in the extended form, as in panel (A). (C) The L1 loop in the retracted

663 form. The figures were made with PyMOL (Schrödinger, LLC) from PDB structure 3Q05; for a  
664 detailed description of the p53 DNA-protein interaction see <sup>44,45,46</sup>.

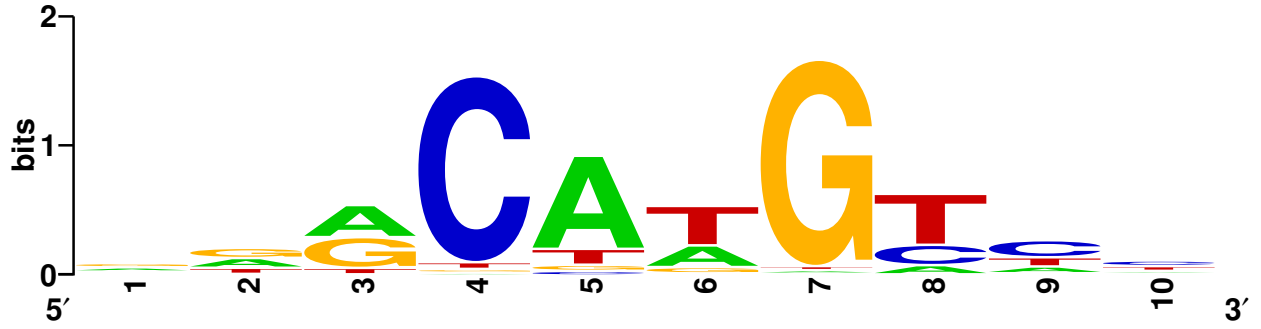




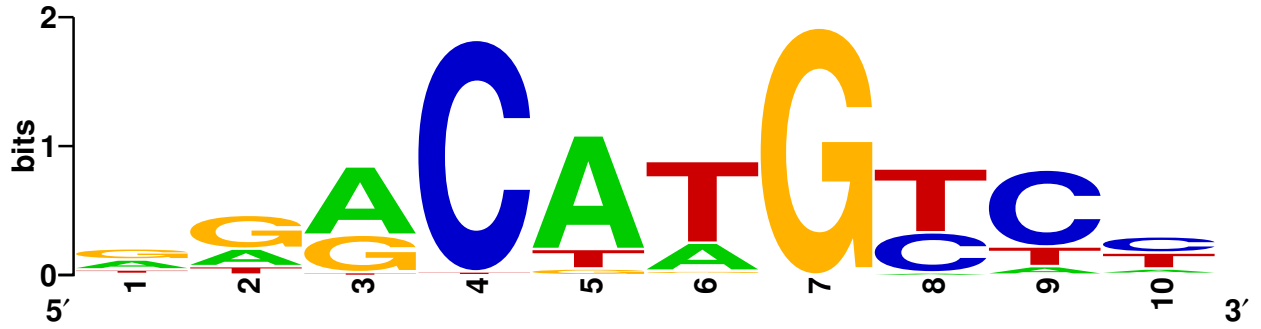
(A) Cluster 1



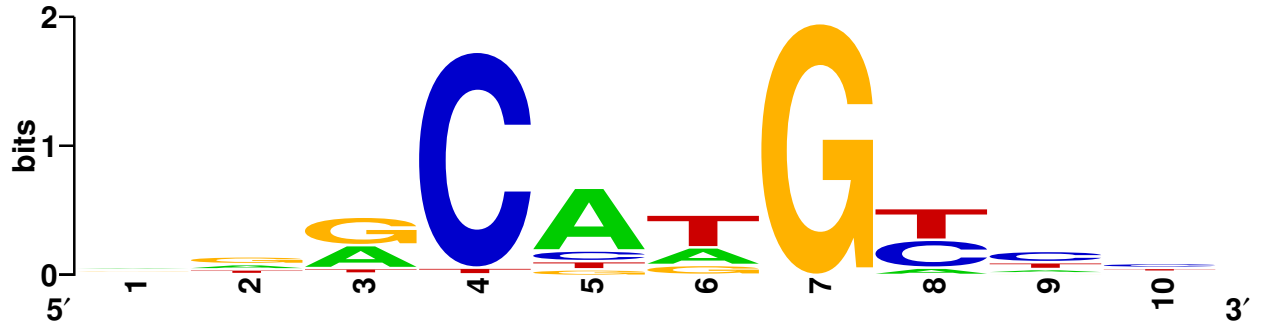
(B) Cluster 2



(C) p53 (Transfac)

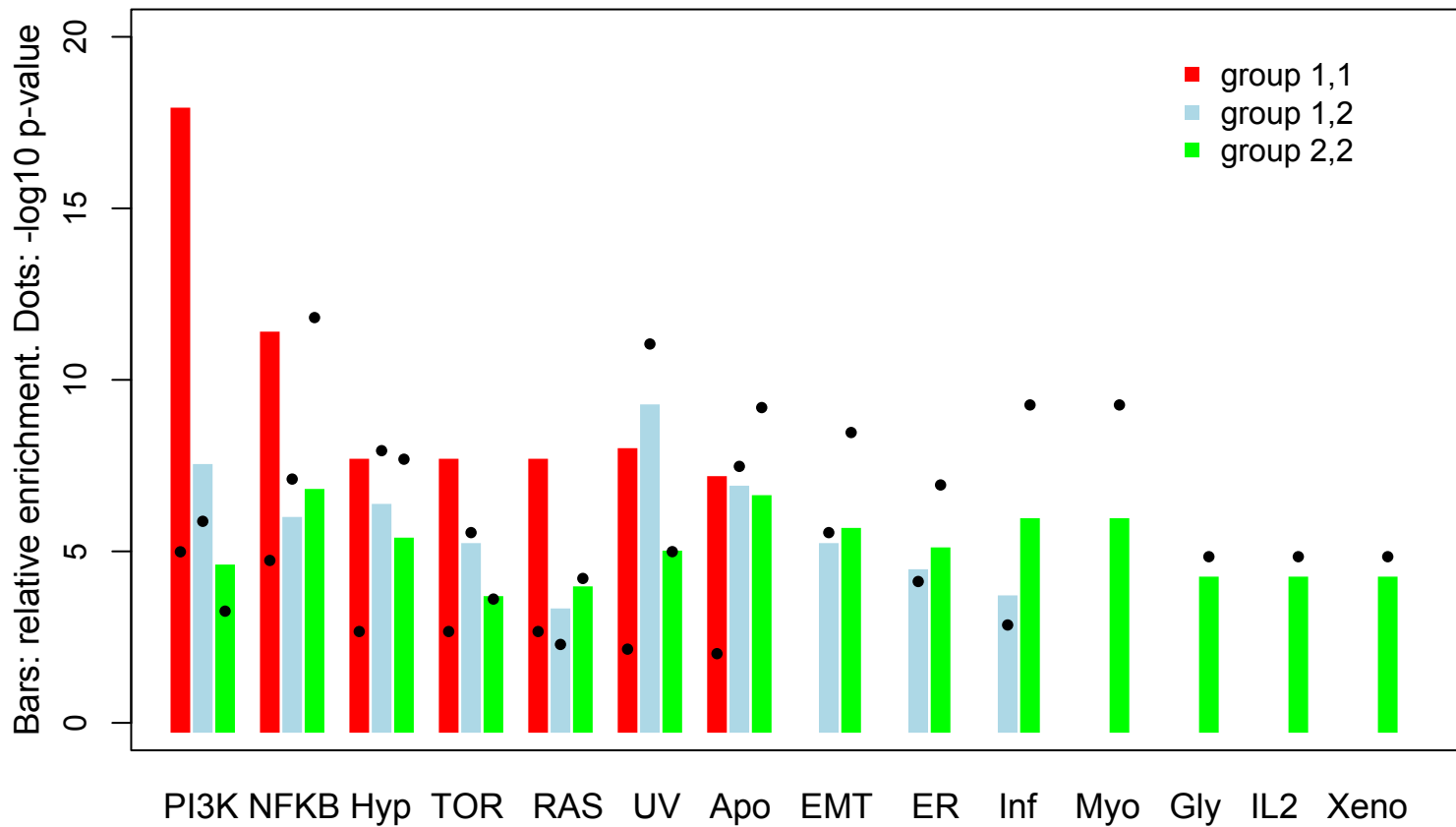


(D) p63

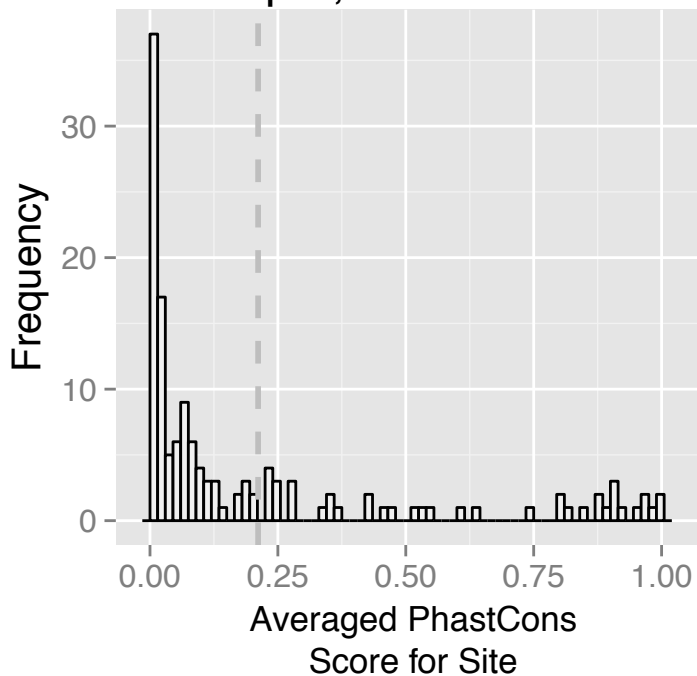


(E) p73

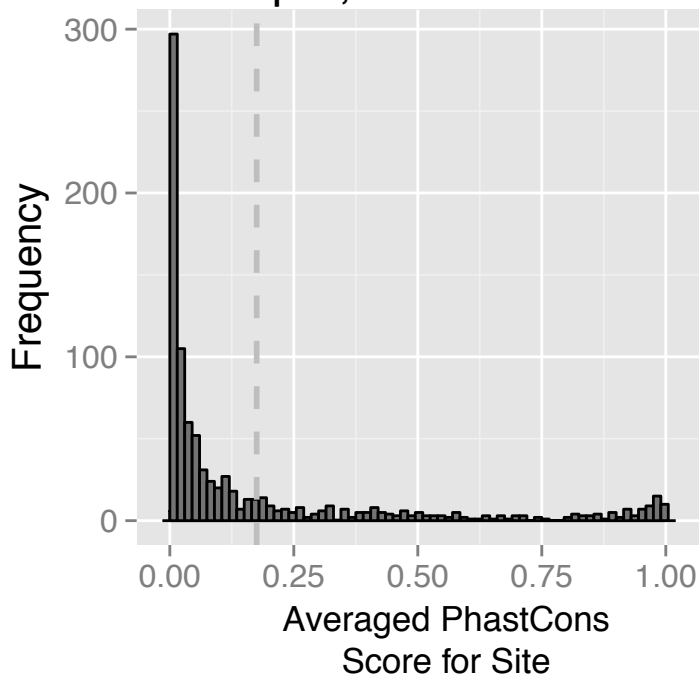




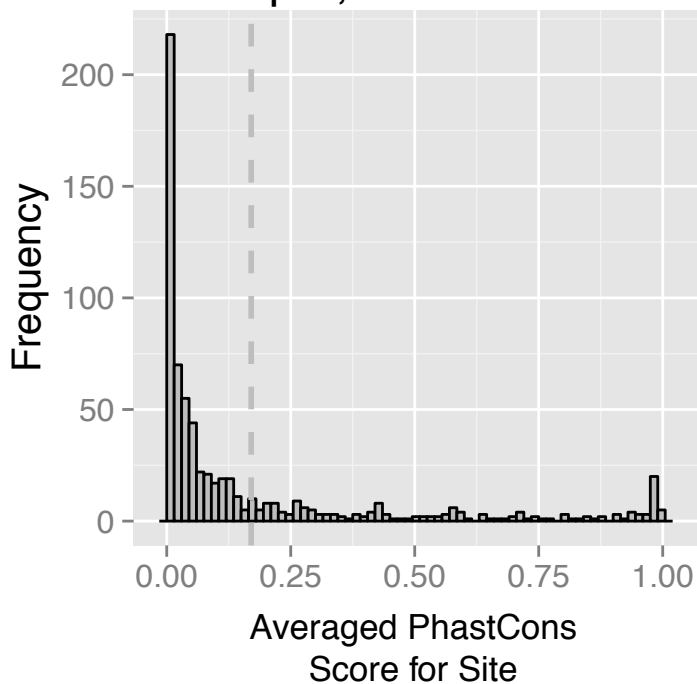
### Group 1,1 Conservation



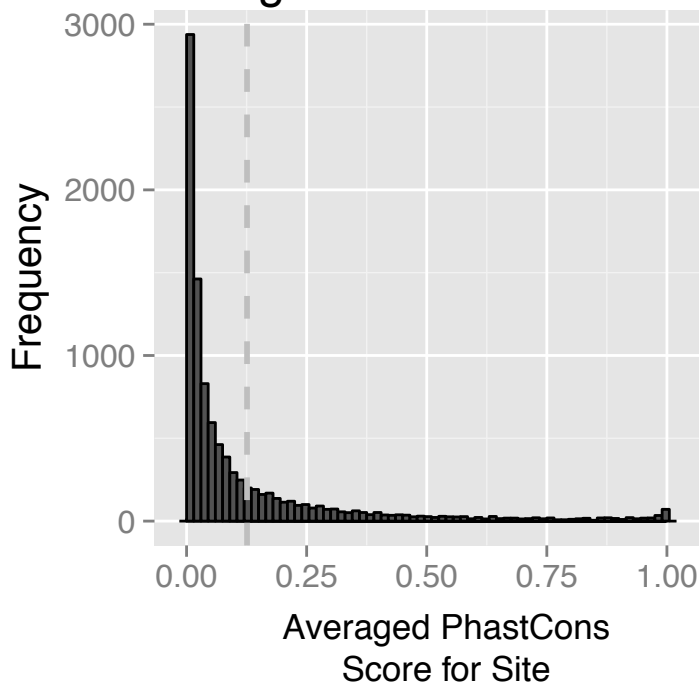
### Group 2,2 Conservation



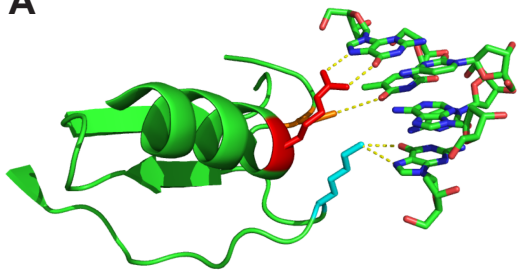
### Group 1,2 Conservation



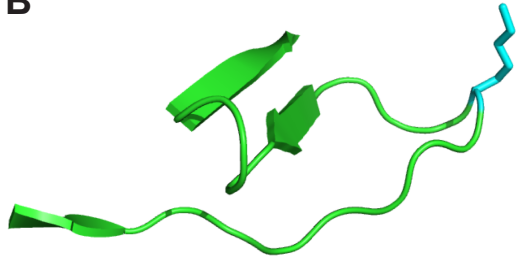
### Background Conservation



**A**



**B**



**C**

